Proposal to Generate an Isolated Monocycle X-Ray Pulse by Counteracting the Slippage Effect in Free-Electron Lasers

Takashi Tanaka*
RIKEN SPring-8 Center, Koto 1-1-1, Sayo, Hyogo 679-5148, Japan
(Received 30 September 2014; published 26 January 2015)

A novel scheme is proposed to generate an isolated monocycle x-ray pulse in free-electron lasers, which is based on coherent emission from a chirped microbunch passing through a strongly tapered undulator. In this scheme, the pulse lengthening by optical slippage, being intrinsic to the lasing process of free-electron lasers, can be effectively suppressed through destructive interference of electromagnetic waves emitted at individual undulator periods. Calculations show that an isolated monocycle x-ray pulse with a wavelength of 8.6 nm and a peak power of 1.2 GW can be generated if this scheme is applied to a 2-GeV and 2-kA electron beam.

DOI: 10.1103/PhysRevLett.114.044801 PACS numbers: 41.60.Cr, 42.55.Vc

Shortening the laser pulse is of great importance to study the dynamics of ultrafast processes because its temporal resolution is specified by the pulse length, which can be theoretically reduced down to one wavelength (monocycle). Nowadays, techniques to generate the monocycle pulses have become mature in visible and infrared regions, and intense laser pulses with the length of several femtoseconds are readily available.

If the monocycle-pulse generation can be applied to shorter-wavelength (x-ray) lasers available in free-electron laser (FEL) facilities [1–4], the pulse length can get down to several attoseconds to hundreds of zeptoseconds, which makes it possible to probe the ultrafast dynamics that is too fast to be investigated with long-wavelength (LW) lasers. In practice, however, the shortest pulse length currently available in x-ray FELs still remains comparable to that of LW lasers.

In order to further shorten the x-ray pulse in FELs, a lot of ideas have been proposed to date [5–17]. In addition, novel schemes to compress the x-ray pulse [18], and to generate few-cycle pulse trains [19], have been recently proposed. Note, however, that there have been no ideas and technologies to shorten the pulse length to the theoretical limit and generate an isolated monocycle x-ray pulse.

It is well known that the microbunch, or the density modulation regularly spaced with an interval of the laser wavelength λ, is the source of lasing in FELs. Thus, the laser pulse length l_L strongly depends on the microbunch length $l_b = M\lambda$, where M is the number of density modulation; if M is reduced in some way and l_b is shortened, so is l_L. It is easy to understand that the minimum of l_b is λ ($M = 1$), in which case a monocycle microbunch is formed in the electron beam. On the other hand, l_L can never get down to λ, even if l_b approaches λ. This comes from the slippage effect in the electron beam moving in an undulator, in which the optical pulse overtakes electrons by λ while they travel one undulator period. To be more specific, the laser pulse generated by the monocycle microbunch passing through an N-period undulator has the pulse length corresponding to N cycles. In other words, a monocycle laser pulse can be generated by combining the monocycle microbunch with a single-period ($N = 1$) undulator, in which case the laser peak power is significantly limited.

In this Letter, we propose a new scheme to generate an intense monocycle pulse with an N-cycle microbunch passing through an N-period undulator, where N is much larger than unity. The point is that the interval of density modulation linearly changes with the longitudinal coordinate along the electron beam ("chirped microbunch") and the undulator is properly tapered; i.e., the field strength linearly changes.

Let us first explain the principle of operation. We consider an electron beam having a chirped microbunch with ten cycles, whose current profile is schematically illustrated in Fig. 1(a). The coordinate $s = c(z/\bar{v}_z - t)$ denotes the longitudinal position relative to a certain reference point in the electron beam, where c, z, t, and $\bar{v}_z$ denote the speed of light, longitudinal coordinate, time, and average velocity of the electron beam in the longitudinal direction, respectively. The distance λ_n denotes the interval of density modulation that linearly changes as s. The electron beam passes through a ten-period tapered undulator, whose field strength changes along the longitudinal axis so that the fundamental wavelength at the nth period coincides with λ_n. In order to facilitate the following discussions, let us define the origin of s as the tail end of the microbunch, which is indicated by the dashed line.

The electric field of radiation emitted at the first period reflects the profile of the chirped microbunch, as in Fig. 1(b). The radiation pulse emitted by the tail end of the microbunch at the first period is hereinafter referred to as the resonant pulse, whose position is indicated by an arrow. Because of the slippage effect, the radiation pulse is

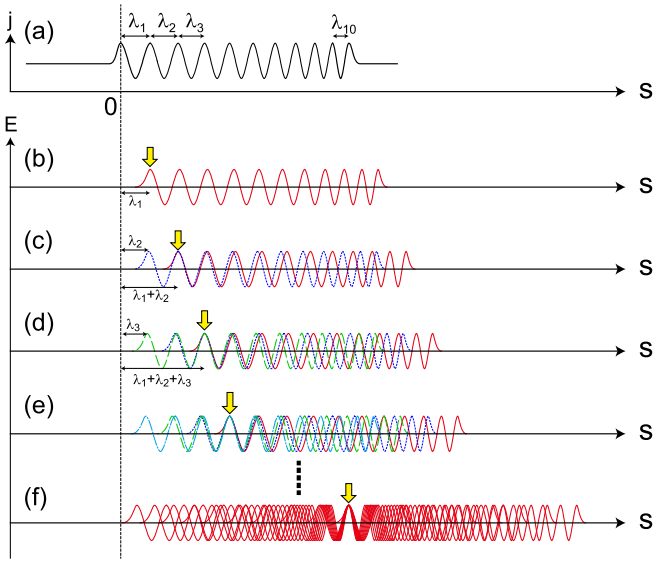

FIG. 1 (color online). Mechanism to generate a monocycle pulse from the chirped microbunch.

shifted forward by the distance of λ_1. As a result, the resonant pulse is located at $s = \lambda_1$.

Figure 1(c) shows the field profile of radiation emitted at the second period (dotted blue line) together with that emitted at the first period and shifted forward because of the slippage effect (solid red line). Note that the slippage length at this period is λ_2, and the resonant pulse is located at $s = \lambda_1 + \lambda_2$ but not at $s = 2\lambda_1$. It is easy to understand that the interference at the resonant pulse is constructive, which is not necessarily the case for other positions. This discussion also applies at the third [Fig. 1(d)] and fourth [Fig. 1(e)] periods, in which the field profiles of radiation emitted at the respective periods are indicated by the dashed green and cyan chain lines, respectively.

Figure 1(f) shows the field profiles of radiation emitted over the whole periods, which are now indicated by solid red lines. We find that the interference at the resonant pulse is completely constructive, while those at other positions are rather destructive. Summing up all the profiles, an intense monocycle pulse is generated at the resonant pulse.

The above explanations are mathematically validated as follows. The electric field of coherent radiation emitted by the chirped microbunch passing through a tapered undulator $E(t)$ is given by the convolution of two functions $n(t)$ and $E_s(t)$, i.e., $E(t) = n(t) \otimes E_s(t)$, with $n(t) = n_0[1 + bf(t)]$ being the temporal profile of the chirped microbunch and $E_s(t) = E_0 g(t)$ being the electric field of radiation emitted by a single electron passing through the undulator. Here, $f(t)$ and $g(t)$ refer to a chirped sinusoid, n_0 denotes the average electron density, b denotes the microbunch factor satisfying $|b| \leq 1$, and E_0 denotes the field amplitude.

Now, let us recall the condition that the fundamental wavelength at the nth period coincides with λ_n, which mathematically imposes $g(t) = f(T - t)$, where T is an arbitrary time. Redefining the origin of t, we have $E(t) = bn_0 E_0 \mathcal{F}^{-1}[|\tilde{f}(\omega)|^2]$, where $\mathcal{F}^{-1}$ denotes the inverse Fourier transform and $\tilde{f}(\omega)$ is the Fourier transform of $f(t)$. The above equation suggests that $E(t)$ is given by the inverse Fourier transform of the spectral function of tapered undulator radiation, i.e., $|\tilde{f}(\omega)|^2$. Taking into account the fact that $|\tilde{f}(\omega)|^2$ is a smooth function of ω having a wide bandwidth depending on the taper rate, it is easy to understand that the temporal width of $E(t)$ can be shorter by applying a larger taper rate. In other words, the pulse length can be controlled by tuning the taper rate, and ultimately, an isolated monocycle radiation pulse can be generated. Note that the condition $g(t) = f(T - t)$ may not be exactly fulfilled in reality; however, the above conclusion does not significantly change as discussed later.

Next, practical procedures to realize the above concept are presented using Fig. 2, where the schematic layout of undulators and related components is shown. This is similar to what is used in the so-called high gain harmonic generation (HGHG) FEL [3,20] but differs from that in the point that (1) the pulse length of the seeding light should be ultimately short, i.e., monocycle or at least a few cycles, and (2) the radiator should be a tapered undulator.

The arrows indicated by the numbers from (i) to (v) show the five sections in charge of respective processes, which are important for this scheme to work. In what follows, each process is explained using Fig. 3, where the typical current profile and electric field in the time domain are shown at the longitudinal positions from (0) to (5), corresponding to the entrances and exits of respective sections.

In section (i), an undulator (modulator) with a single period followed by a chicane (dispersive section) is installed, which induces an energy modulation in the electron beam and converts it to the density modulation. As a result, an isolated monocycle microbunch is generated when the monocycle seed pulse at the wavelength of λ_0 is injected synchronously with the electron beam. The peak power of the seed pulse should be high enough to create a

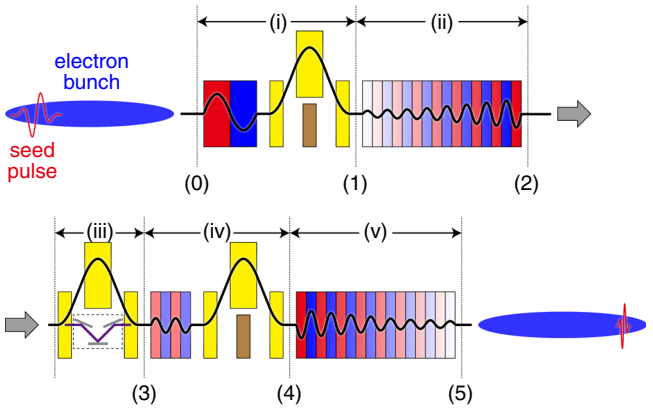

FIG. 2 (color online). Layout of the undulators and chicanes for the MCHG scheme.

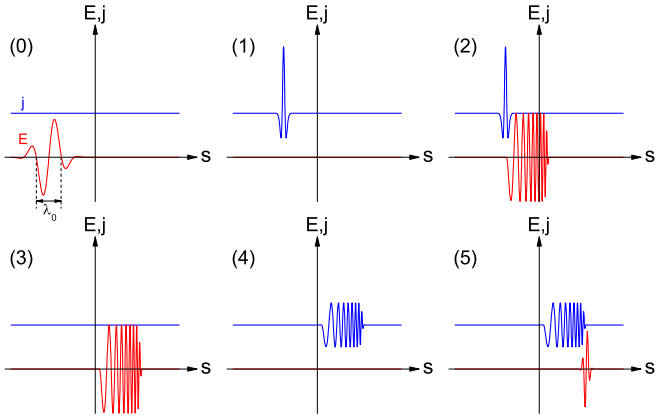

FIG. 3 (color online). Schematic illustration of the current profiles (j) and electric field distributions (E) at the borders between different sections.

monocycle microbunch with strong harmonic components, which is crucial for this scheme to work. In addition, an optical shutter is inserted in the chicane to eliminate the seed pulse, which is not necessary anymore in the following sections. As shown in Fig. 3, positions (0) and (1), a monocycle electric field is present and the beam current is constant at the entrance (0), while the seed pulse is eliminated and the monocycle microbunch is produced at the exit (1), with the length much shorter than λ_0.

In section (ii), the monocycle microbunch is injected to the tapered undulator (radiator), whose K value linearly changes as $K[1 + (\Delta K/K)\Delta z/L]$, and emits chirped radiation as shown in Fig. 3, position (2). Here, Δz denotes the longitudinal distance relative to the undulator center and L denotes the undulator length. The average K value (K) is tuned so that the central wavelength of radiation corresponds to λ_0/m, where m is the target harmonic number. It is worth noting that the chirped radiation generated in this process may be compressed, if an appropriate dispersive optics is available in the wavelength region around λ_0/m, which is a common method in LW lasers.

In section (iii), the electron beam passes through a chicane so that the microbunches created in the former processes are washed out and the generated chirped radiation is sent forward to the position where the electrons are still "fresh," as shown in Fig. 3, position (3). This is known as the fresh-bunch technique [21]. In case the dispersive strength to wash out the microbunch and the resultant optical slippage are so large that the chirped radiation slips out of the electron beam, the optical delay chicane [22] composed of simple plane mirrors to retard the radiation, which is indicated by the dashed rectangle, can be utilized in order to adjust the timing between the electron beam and the chirped radiation.

In section (iv), a "chirped microbunch" is formed in the electron beam, as shown in Fig. 3, position (4), through interaction with the chirped radiation generated in the previous process. For this purpose, an undulator (modulator) with a few periods and appropriate parameters (period and K value) is installed, followed by a chicane (dispersive section) with an optical shutter as in section (i).

In section (v), the chirped microbunch is injected to the tapered undulator (radiator) having the identical specifications to those used in section (ii) except that the taper direction is reversed. This is to make sure that the profile of the chirped microbunch is similar to that of the electric field of tapered undulator radiation except the time reversal. Based on the principle already explained, an isolated monocycle pulse with the wavelength of λ_0/m is generated as shown in Fig. 3, position (5).

Obviously, the above scheme works to up-convert the input monocycle seed pulse and thus is hereinafter referred to as the monocycle harmonic generation (MCHG). It is worth mentioning that the MCHG scheme can be cascaded for further shortening the wavelength, by utilizing the produced monocycle pulse as the seed of the next stage, as long as its peak power is sufficiently high. This corresponds to the scheme known as the cascaded HGHG [21]. Note that a chicane should be inserted between stages as in the fresh-bunch chicane [section (iii)].

In order to investigate the feasibility and performance of MCHG, we developed a simulation code to solve the FEL equations with the diffraction and space-charge effects taken into account, which assumes an axial symmetry but does not take advantage of common numerical methods such as averaging over the undulator period and slicing with the laser wavelength. This is because the validity of applying these methods to the process of coherent emission from the chirped microbunch is not obvious. The developed code was then benchmarked by comparing with the existing code for the normal HGHG processes without undulator tapering, and we found that the results were consistent.

Using the developed code described above, the process of MCHG has been simulated under an assumption that a 2-GeV electron beam with the constant current of 2 kA and normalized emittance of 0.4 μm is injected to the undulator

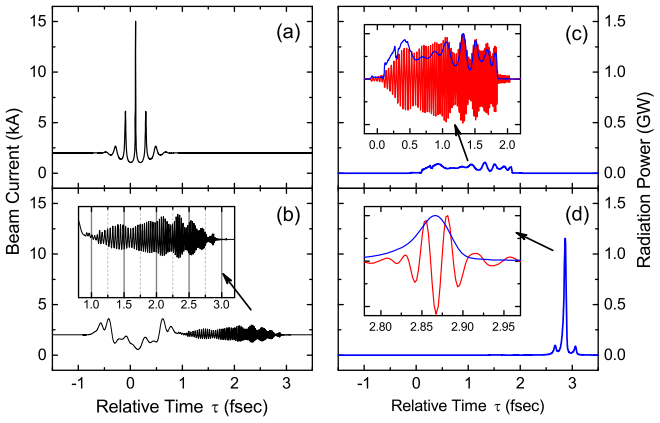

FIG. 4 (color online). Simulation results for $n = 7$ (8.6 nm), $\sigma_\gamma/\gamma = 5 \times 10^{-5}$, and $\Delta K/K = 0.5$.

TABLE I. Parameters for the undulator and dispersive sections assumed in Fig. 4; λ_u, N, and K denote the period length, period number, and K value of the undulators, and R_{56} denotes the dispersive strength.

Section	λ_u (mm)	N	K	R_{56} (mm)
(i)	170	1	3.13	0.015
(ii),(v)	27	60	2.21–3.69	…
(iii)	…	…	…	0.20
(iv)	81	2	1.39	0.024

section with the average betatron function of 4 m, synchronously with the seed pulse having the central wavelength of 60 nm, pulse energy of 10 μJ, and FWHM pulse length of 0.38 fs. It should be emphasized that generation of such an intense attosecond pulse has been demonstrated and reported in Ref. [23]. The simulation has been repeated for different values of harmonic number (m) and energy spread of the electron beam (σ_γ/γ). As an example, the result for a particular case of $m = 7$ (8.6 nm), $\sigma_\gamma/\gamma = 5 \times 10^{-5}$, and the taper rate of $\Delta K/K = 0.5$ is shown in Fig. 4, with relevant parameters summarized in Table I.

Note that utilization of helical undulators is supposed for a better interaction efficiency between radiation and electrons. In addition, the undulator K value in section (iv) is detuned from the nominal value of 1.50. This is to enhance the energy modulation induced by the shorter-wavelength region of chirped radiation, which eventually results in shortening the pulse length in this particular example, slightly at the expense of the peak power.

In Figs. 4(a) and 4(b), the beam current profiles are plotted at the entrances of two tapered undulators, i.e., at positions (1) and (4) indicated in Fig. 2, respectively. The abscissa is given by the relative time $\tau = s/c$, and its origin is defined as that of the seed pulse when it arrives at the entrance of section (i), i.e., position (0). In Figs. 4(c) and 4(d), the temporal profiles of radiation power at the exits of two undulators are plotted, together with the normalized electric field of radiation in insets.

Now, let us take a look at how the monocycle pulse is generated, using Figs. 4(a)–4(d). At the exit of section (i), a monocycle microbunch having the peak current of 15 kA is created (a), which passes through the first tapered undulator (ii) and emits the chirped radiation (c). Then, in section (iv), the chirped radiation is converted to the chirped microbunch (b), which passes through the second tapered undulator to generate an isolated monocycle pulse with the peak power of 1.2 GW and FWHM pulse length of 0.046 fs as shown in (d), which corresponds to 1.6 cycles at 8.6 nm. It is worth mentioning that the saturation power in the regular FEL process with the parameters under consideration is around 10 GW, and thus, the MCHG process is not saturated in this example.

We find in Fig. 4(b) that the monocycle microbunch created in the earlier process still remains as the density

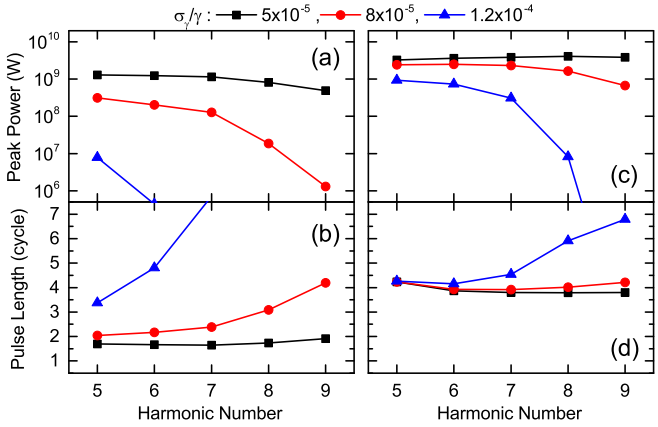

FIG. 5 (color online). (a),(c) Peak power and (b),(d) pulse length plotted as a function of m for different values of σ_γ/γ.

modulation (around $\tau = 0$), even after the chicane (iii) inserted to wash out the microbunch. This modulation, however, has a typical frequency much lower than that of the chirped microbunch and thus has no impact in the following processes. In addition, the radiation temporal profile after the first tapered undulator shown in (c) has fine structures coming from the secondary current spikes as found in (a).

Figures 5(a) and 5(b) show the peak power and pulse length of radiation, respectively, which are retrieved from the results of simulations performed with different values of m and σ_γ/γ. Note that the pulse length is given as the number of cycles, namely, normalized by the wavelength at the mth harmonic, and the electron energy, undulator K values in section (i), and dispersive strengths have been adjusted appropriately for respective harmonics, but other undulator parameters are kept constant.

When the energy spread is small ($\sigma_\gamma/\gamma = 5 \times 10^{-5}$), the MCHG scheme works well; the peak power reaches around 1 GW with the pulse length less than two cycles for the harmonics up to the ninth (6.7 nm). The performance, however, drops rapidly as the energy spread increases, which makes the MCHG scheme almost impractical when $\sigma_\gamma/\gamma = 1.2 \times 10^{-4}$, with the parameters currently under consideration. This is because the energy modulation induced in section (iv) is not large enough to overcome the effects due to the energy spread of the electron beam [20] and create the chirped microbunch.

We have two possible solutions against the above problem. One is to increase the undulator periods in section (iv) ($= N^{(\mathrm{iv})}$), and the other is to reduce the undulator taper ($\Delta K/K$). For example, Figs. 5(c) and 5(d) show the simulation results when $N^{(\mathrm{iv})}$ is increased from 2 to 4 and $\Delta K/K$ is reduced from 0.5 to 0.2. We find that the peak power is significantly enhanced by these modifications, albeit at the expense of lengthening the pulse length, and now the MCHG scheme works reasonably well even with $\sigma_\gamma/\gamma = 1.2 \times 10^{-4}$.

*ztanaka@spring8.or.jp

[1] P. Emma *et al.*, Nat. Photonics **4**, 641 (2010).
[2] T. Ishikawa *et al.*, Nat. Photonics **6**, 540 (2012).
[3] E. Allaria *et al.*, Nat. Photonics **6**, 699 (2012).
[4] M. Vogt *et al.*, in *Proceedings of the 5th International Particle Accelerator Conference, Dresden, Germany, 2014* (JACoW, Geneva, Switzerland, 2014), p. 938.
[5] E. L. Saldin, E. A. Schneidmiller, and M. V. Yurkov, Opt. Commun. **212**, 377 (2002).
[6] P. Emma, K. Bane, M. Cornacchia, Z. Huang, H. Schlarb, G. Stupakov, and D. Walz, Phys. Rev. Lett. **92**, 074801 (2004).
[7] S. Reiche, P. Musumeci, C. Pellegrini, and J. B. Rosenzweig, Nucl. Instrum. Methods Phys. Res., Sect. A **593**, 45 (2008).
[8] Y. Ding *et al.*, Phys. Rev. Lett. **102**, 254801 (2009).
[9] E. L. Saldin, E. A. Schneidmiller, and M. V. Yurkov, Opt. Commun. **239**, 161 (2004).
[10] A. A. Zholents and W. M. Fawley, Phys. Rev. Lett. **92**, 224801 (2004).
[11] A. A. Zholents, Phys. Rev. ST Accel. Beams **8**, 040701 (2005).
[12] A. A. Zholents and G. Penn, Phys. Rev. ST Accel. Beams **8**, 050704 (2005).
[13] E. L. Saldin, E. A. Schneidmiller, and M. V. Yurkov, Phys. Rev. ST Accel. Beams **9**, 050702 (2006).
[14] W. M. Fawley, Nucl. Instrum. Methods Phys. Res., Sect. A **593**, 111 (2008).
[15] A. A. Zholents and M. S. Zolotorev, New J. Phys. **10**, 025005 (2008).
[16] D. Xiang, Z. Huang, and G. Stupakov, Phys. Rev. ST Accel. Beams **12**, 060701 (2009).
[17] Y. Ding, Z. Huang, D. Ratner, P. Bucksbaum, and H. Merdji, Phys. Rev. ST Accel. Beams **12**, 060703 (2009).
[18] T. Tanaka, Phys. Rev. Lett. **110**, 084801 (2013).
[19] D. J. Dunning, B. W. J. McNeil, and N. R. Thompson, Phys. Rev. Lett. **110**, 104801 (2013).
[20] L. H. Yu, Phys. Rev. A **44**, 5178 (1991).
[21] I. Ben-Zvi, K. M. Yang, and L. H. Yu, Nucl. Instrum. Methods Phys. Res., Sect. A **318**, 726 (1992).
[22] G. Geloni, V. Kocharyan, and E. Saldin, DESY Report No. 10-004.
[23] E. J. Takahashi, P. Lan, O. D. Muecke, Y. Nabekawa, and K. Midorikawa, Nat. Commun. **4**, 2691 (2013).